Transactions of the Materials Research Society of Japan 25 [4] 1191-1194 (2000)

Thermostability and Structural Model Calculation of Antibacterial and Antifungal Agents Derived from Clay Minerals

Fumihiko Ohashi, Masaya Suzuki, Shinji Tomura, Asao Oya*,
Laurent Duclaux** and Francois Beguin**
Ceramic Technology Deartment, National Industrial Research Institute of Nagoya, AIST, MITI
1-1 Hirate, Kita, Nagoya, 462-8510, JAPAN
Fax: +81-52-916-6993, e-mail: fohashi@nirin.go.jp
*Faculty of Engineering, Gunma University
1-5-1 Tenjin, Kiryu 376-0052, JAPAN
**CRMD-CNRS, Universite d'Orleans
1B, rue de la Ferollerie-45071, Orleans Cedex 2, FRANCE

The authors have been reported montmorillonite intercalated by silver chelate of 2-(4-thiazolyl)-benzimidazole (TBZ) that has strong antimicrobial and antifungal activities. However, the structure of the silver chelate intercalated montmorillonite and their thermostabilities have not been determined. In this study, the resulting samples were subjected to examination of their thermostabilities by thermogravimetry and carbon dioxide evolution analyses up to 500°C in air. On the other hand,Na-montmorillonite and Li-taeniolite were intercalated by the silver chelate of TBZ, and their structural model calculation were carried out. The structure of the resulting films were derived from the (00*l*) relative intensities observed by X-ray diffraction. The thermal degradation behavior of the intercalants were significantly changed by intercalating between the montmorillonite layers. The TBZ was released from the montmorillonite around at 370°C, which temperature was higher than that for the TBZ itself. Structural model calculation on the resulting intercalated clay film indicated that the silver chelate was oriented vertically between the layers of montmorillonite with its extremities at the center of the ditrigonal cavities. The improvement of the thermostability after intercalation can be attributed to the bonding between the intercalant and the host montmorillonite layers.
Keywords: Clay minerals, Thermostability, Structural model calculation

1. INTRODUCTION

It is well known that a number of clay minerals have a layer structure which can accept organic and/or inorganic cations within their interlayer space by an exchange reaction. For example, all sorts of quaternary alkylammonium cations were representative guest species among a variety of the reported ones[1]. The authors have been attempting to prepare antimicrobial and antifungal agents derived from clay minerals by cation exchange, and have previously studied the properties of the silver cation or silver chelate intercalated montmorillonite. This technique was further extended to prepare an agent with both strong antibacterial and antifungal activities. For instance, the authors showed a montmorillonite intercalated by silver chelate of 2-(4-thiazolyl)-benzimidazole (TBZ) which has strong antimicrobial and antifungal activities[2]. There is the possibility that this intercalation technique using montmorillonite as a host material can be employed to prepare an antimicrobial agent with high thermostability.

In the present work, the thermostabilities of montmorillonite intercalated by a silver chelate of TBZ and the arrangement of the silver chelate between the silicate layers were determined. Thermostability was estimated by analyses of thermogravimetry and evolved carbon dioxide gas up to 500°C in air. For the structural model calculation, Li-taeniolite and Na-montmorillonite were used as the hosts to intercalate the silver chelate. As the degree of parallel layer stacking order in taeniolite is higher than that in montmorillonite, the former may be available for structural model calculation. The structure of the mineral-silver chelate intercalation complex was studied by X-ray diffraction. By comparing the calculated intensities of the (00*l*) lines to the measured counterparts, the arrangement of the silver chelate between the silicate layers was estimated.

2. EXPERIMENTAL

2.1. Materials

Li-taeniolite with the chemical formula of $LiMg_2Li(Si_4O_{10})F_2$ was supplied by Topy Ind. Co. Na-montmorillonite was provided by Kunimine Ind. Co., and has the typical chemical formula of $Na^{0.66+}[(Al_{3.33}Mg_{0.67})(Si_8O_{20})(OH)_4]^{-0.66}$.

Table I. Characteristic data of the clay minerals.

	SSA* (m^2/g)	CEC (cmol(+)/kg)	PA** (nm^2)
Li-taeniolite	620	260	0.20
Na-montmorillonite	750	108	0.58

*Specific surface area by BET plots.
**Projected area available for one positive charge.

The cation exchange capacity (CEC) and specific surface area of the minerals together with projected area of one exchangeable cation are summarized in Table I. The chelating agents were 2-(4-thiazolyl)-benzimidazole ($C_{10}H_7N_3S$) and silver nitrate ($AgNO_3$).

2.2. Synthesis

A 2mass% clay mineral water suspension was shaken for 2days, and the clay mineral sol was spread on a plastic plate with a flat surface and dried at room

temperature for 7days. The air-dry clay mineral film (0.1g) on the plastic plate was placed in a beaker equipped with magnetic hot plate. Silver nitrate and TBZ were dissolved in deionized water by 3molar quantity of the CEC of the montmorillonite and in methanol by 6molar quantity of the CEC, respectively. The two solutions were then mixed together at room temperature to form the white suspension of the Silver TBZ chelate, $Ag^{+}(TBZ)_2NO_3^{-}$. The chelate suspension was then added to the beaker containing the clay mineral film (3moles of chelate for 1mole of exchangeable cation), and kept at 60°C for 3days with stirring for the cation exchange reaction to take place. The resulting clay mineral film intercalated with the $Ag(TBZ)_2$ chelate was then repeatedly washed with deionized water to remove the free chelate. After that, the intercalated film was dried at room temperature on a glass plate.

2.3. Characterization

The identity period was determined by X-ray diffraction from average on several orders of the (00*l*) peaks using a Siemens D-500 diffractometer with the Ni-filtered Cu-Kα radiation. Carbon content was measured by a carbon analyzer Horiba EMIA-110.

Using the computer program, LAZY PULVERIX, the calculation of the theoretical X-ray diffraction pattern is as follows. The first routine program (LAZY) gives the parameters of the space group symbol, the coordinates, and chemical symbols of the atoms contained in one elementary unit. The second routine (PULVERIX) calculates the *d* spacings from Bragg's Equation and the positions of the diffraction lines. The diffraction intensity I_{hkl} is calculated as

$$I_{hkl} = M \cdot LP \cdot F^2_{hkl}$$

where M is the multiplicity factor, and LP is the Lorentz Polarization factor for a powder. The structure factor F_{hkl} is defined by

$$F_{hkl} = \Sigma f_j O_j \exp[2\pi i(hx_j+ky_j+lz_j)]\exp[(-B_j\sin^2\theta)/\lambda^2]$$

where f_j is the atomic scattering factor of atom j, O_j is the occupation factor of site x_j, y_j, z_j for atom j, and B_j is the Debye-Waller factor in Å^2 for atom j. The output of the program consists of a listing of *hkl*, *d* spacings, θ values, structure factors and theoretical intensities[3]. The reliability factor, R, for the refinement parameter of the structure model is calculated as follows:

$$R = |\Sigma I_{Obs.} - \Sigma I_{Calc.}| / |\Sigma I_{Obs.}|$$

In our work, $\Sigma I_{Obs.}$ and $\Sigma I_{Calc.}$ are given for the values on the total sum of the observed and calculated (00*l*) relative intensities ($I_{Obs.}$ and $I_{Calc.}$). When R is a minimum close to zero, the structure refinement is considered as achieved. Correct structures usually have R<0.25 and very well refined structures may have R in the neighborhood of 0.05[4].

Thermogravimetric (TG) measurement and evolved carbon dioxide gas analysis were conducted using a thermogravimeter TAS-200 TG8110D (Rigaku Electrical Co., Ltd.). The sample of 40mg was heated to 500°C at a rate of 5°C/min in a stream of air (60ml/min). The evolution rate of carbon dioxide was measured at intervals of 25°C using a gas chromatography mass spectrometry (GC-3BT, Shimadzu Faculty Co., Ltd.).

3. RESULTS AND DISCUSSION

3.1. Structure of agents

The (00*l*) XRD profiles of Li-taeniolite and Na-montmorillonite are shown in Fig.1. The original taeniolite film showed a strong (001) diffraction peak and higher order reflections, indicating a basal spacing at 1.23nm characteristic of a single water layer type structure for a 1.0nm basal spacing mineral[5]. In the case of the montmorillonite film, the relatively narrow (001) peak at about 7° and the higher order lines showed a well orientated material with a basal spacing (1.25nm) indicating a one layer hydrated type material[5].

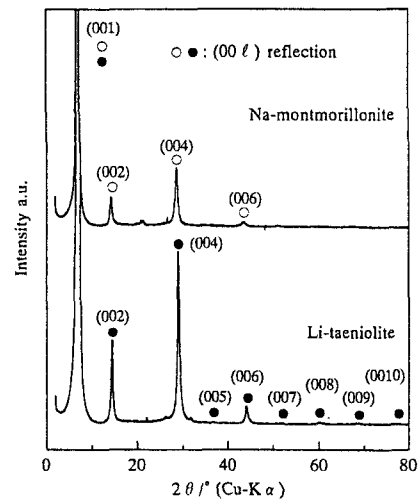

Fig.1. X-ray diffraction profiles of the clay minerals.

The configuration of the $Ag^{+}(TBZ)_2$ chelate with its dimensions along typical directions and the XRD profiles of the $Ag(TBZ)_2$-montmorillonite and $Ag(TBZ)_2$-taeniolite are shown in Fig.2. As shown in Tables I and II, the projected area available for one positive charge in clay minerals are respectively 0.20 and 0.58nm^2, whereas the chelate projected area is in the range 0.33 to 0.45nm^2 These values were calculated from the thickness (0.35nm) and the planer configuration of the chelate. From these comparisons, incomplete exchange of the chelate with the Li-taeniolite would be expected due to the discrepancy between the available area for one positive charge and the dimension of the $Ag^{+}(TBZ)_2$ cation. On the other hand, montmorillonite will be suitable for the cation exchange with the bulky $Ag^{+}(TBZ)_2$ cation because of its high available projected area for one positive charge.

The diffraction pattern (Fig.2(a)) of the $Ag(TBZ)_2$-montmorillonite film produced only sharp (00*l*) reflections suggesting a parallel orientated structure. However the *d*-spacing deduced for each reflection presented slight fluctuations characteristic of some intervals with different thickness. The average interlayer spacing deduced from all the (00*l*) lines is close to 2.01nm. According to the carbon analysis, $Ag^{+}(TBZ)_2$ chelate was intercalated between the montmorillonite layers in amount of 95%.

The XRD profile of the $Ag(TBZ)_2$-taeniolite film (Fig.2(b)) could not be interpreted as that of a pure compound, but rather a mixture of two phases with average interlayer spacing of 2.03nm and 1.45nm, respectively. The first period is comparable to the one which was found in the case of $Ag(TBZ)_2$-montmorillonite at 2.01nm and could be attributed to the intercalation of $Ag^{+}(TBZ)_2$ in the interlayer space. The

additional basal spacing at 1.45nm could be due to the existence of a double layer of Li^+-hydrating molecules[5], whose diffusion outside of the interlayer space is blocked by the presence of the bulky $Ag^+(TBZ)_2$ cations at the boundary of the intercalated islands.

Table II Dimension of the Ag-TBZ chelate along the *c* direction and its projected area on the basal plane.

	Axis parallel to *c* length(nm)	Projected area (nm^2)*
A	0.92	0.44
B	1.23	0.33
C	1.25	0.40
D	1.12	0.45

*The calculated value is an occupation area on vertical standing position for a thickness of 0.36nm.

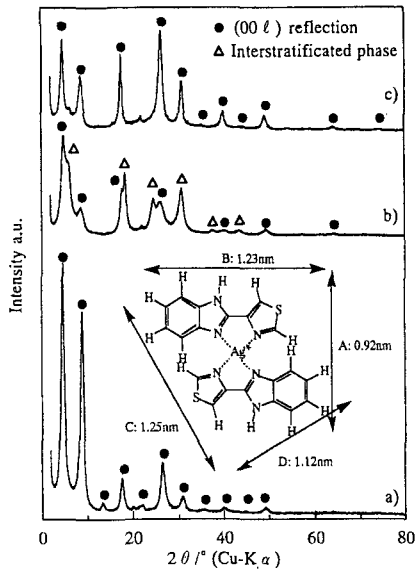

Fig.2. The planner configuration of the $Ag^+(TBZ)_2$ chelate and the XRD profiles of the (a)$Ag(TBZ)_2$-mont-morillonite, (b)$Ag(TBZ)_2$-taeniolite for the first exchange 3days at 60°C and (c)for second exchange 3days at 60°C.

To confirm this interpretation, additional exchange with a fresh suspension of $Ag^+(TBZ)_2NO_3^-$ chelate (3times the CEC of the untreated taeniolite) was performed during 3days at 60°C. The corresponding X-ray diffractogram (Fig.2(c)) presented only one set of (00*l*) reflections suggesting further exchange. However, some fluctuations were observed both for the position and the width of the low order (00*l*) reflections which is the proof for interstratification, and therefore partial exchange in some intervals. The average interlayer distance was found at 2.03nm, and the comparison with the spectrum of $Ag(TBZ)_2$-montmorillonite (Fig.2(a)) reveals a similar sequence of (00*l*) reflections; only the relative intensities are affected. On the basis of the carbon contents, 86 and 92% of the CEC of the taeniolite were exchanged by the $Ag^+(TBZ)_2$ chelates for first and second exchanged complexes, respectively.

The observed and calculated relative intensities and the R values of the untreated montmorillonite and taeniolite films are shown in Table III. For the taeniolite film there is good agreement between $I_{Obs.}$ and $I_{Calc.}$, giving an R value of 0.02. As regards the montmorillonite film, the comparison of $I_{Obs.}$ to $I_{Calc.}$ produces a good refinement with an R value of 0.08.

Table III The relative intensities of the (00*l*) lines and reliability factor of taeniolite and montmorillonite.

	Li-taeniolite		Na-montmorillonite	
(00*l*)	I_{Obs}	$I_{Calc.}$	$I_{Obs.}$	$I_{Calc.}$
(001)	100	100	100	100
(002)	6.9	9.2	7.0	1.9
(003)	0.0	0.0	0.0	0.0
(004)	11.8	7.4	12.8	9.1
(005)	0.1	0.2	0.0	0.0
(006)	1.7	1.2	1.6	0.3
(007)	0.2	0.2	-	-
(008)	0.3	0.3	-	-
(009)	0.2	0.2	-	-
(0010)	0.1	0.3	-	-
$\Sigma_{Int.}$	121.3	119.0	121.4	111.2
R*	0.02		0.08	

*: Reliability factor
-: Not detected

For the structural model calculation, four arrangements of the chelate have to be considered in terms of the calculated projected area of the chelate standing up vertically on the silicate layers(Fig.2). In the Axis-A arrangement, for example, the A-direction in the chelate is perpendicular to the silicate layers. The calculation of the size in Axis-B, C and D arrangements was carried out in a same manner (see Table II and Fig.2). The (001) basal spacing for each arrangement could be estimated from the van der Waals dimensions of the chelate and the silicate layer thickness (0.94nm). In the Axis-A arrangement the interlayer distance would be 1.86±0.02nm, and 2.17, 2.19 and 2.06±0.02nm respectively for Axis-B, C and D arrangements.

Table IV The relative intensities of the (00*l*) lines of $Ag(TBZ)_2$-montmorillonite depending on the kinds of axis A, B, C or D perpendicular to the silicate layers.

		A	B	C	D
(00*l*)	$I_{Obs.}$	$I_{Calc.}$	$I_{Calc.}$	$I_{Calc.}$	$I_{Calc.}$
(001)	100	100	100	100	100
(002)	82.2	80.7	76.0	87.8	196.6
(003)	3.0	1.5	4.7	13.4	5.7
(004)	13.9	4.0	1.7	4.7	0.4
(005)	2.6	1.3	2.4	3.3	7.3
(006)	24.2	8.4	8.6	6.1	37.5
(007)	6.5	3.4	5.4	4.7	4.2
(008)	1.5	0.1	0.2	0.6	1.1
(009)	2.6	0.7	0.7	0.1	6.1
(0010)	0.8	0.3	0.6	1.7	1.9
$\Sigma_{Int.}$	237.3	207.4	200.3	222.4	360.8
R*		0.13	0.16	0.06	0.52

*: Reliability factor

The four orientations of the chelate in the $Ag(TBZ)_2$-montmorillonite film were assumed for the structural model calculation. For each arrangement the values of $I_{Obs.}$ were compared to those of $I_{Calc.}$ (Table IV). The lowest reliability factor R=0.06 was obtained in the case of the C axis perpendicular to the silicate layers. The magnitude of R supports the validity of the structural modelling of the $Ag(TBZ)_2$-montmorillonite film using this estimation method. The observed (2.01 nm) and calculated (1.25nm+0.94nm=2.19nm) interlayer distances are in reasonably good agreement. To explain the small difference, it is presumed that the two ends of the chelate are embedded in the hexagonal hole of the

montmorillonite interlayer surface. Careful calculations showed that for the C-Axis orientation the chelate is exactly embedded into the center of the ditrigonal cavities in the upper and lower silicate layers. Due to weak interstratification, the observed $d_{(001)}$ may also be slightly smaller than the true identity period, giving rise to some discrepancies between the observed and calculated intensities of some (00*l*) reflections.

In the case of $Ag(TBZ)_2$-taeniolite, however, the comparable sample for the structural model calculation could not be prepared using the Li-taeniolite because of the presence of the interstratificated hydrated phase identified in the X-ray diffraction of the silver chelate-taeniolite intercalated derivative. Comparing the data in Tables I and II, the taeniolite has too small the available projected area to intercalate the silver chelate. The intercalation mechanism between the Li-taeniolite and the silver chelate should be elucidated using other structure models, and especially partial exchange should be taken into account.

3.2. Thermostability of agents

Fig.3 shows the TG curves and the CO_2 evolution rate curves for TBZ, $Ag^+(TBZ)$ chelate and $Ag(TBZ)_2$-montmorillonite in air. TBZ showed a weight loss at 265°C in contrast to 238°C for $Ag^+(TBZ)_2$ chelate. The latter sample showed four weight loss steps at higher temperature. The weight loss of $Ag(TBZ)_2$-montmorillonite was observed at 353°C and proceeded gradually to reach to 24% at 500°C. In the results of gas analysis, an analogous behaviour was observed among three samples, i.e., the gas started to evolve around 400°C and reached a maximum evolution rate at 450°C.

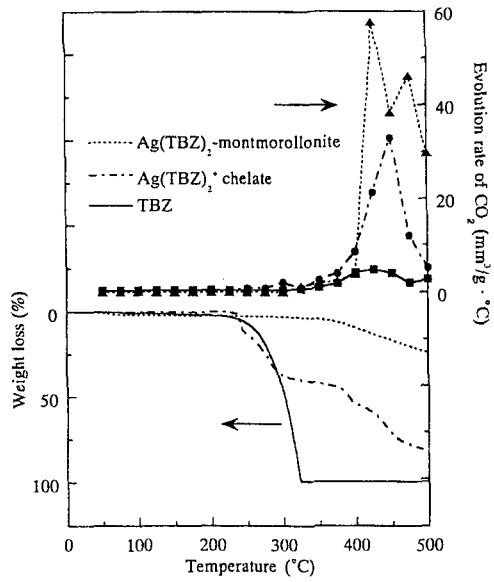

Fig.3. Thermogravimetric and evolution rate of carbon dioxide analyses for the specimens.

The TG measurement showed clearly some significant differences among the thermostabilities of the unchelated organic ligand, its chelate with silver cation and the chelate intercalated between the montmorillonite layers. TBZ showed weight loss at 265°C against 353°C for $Ag(TBZ)_2$-montmorillonite. These phenomena are thought to be dependent on the bonding strength between the montmorillonite layer and the intercalated organic cation in addition to the intrinsic thermostability of the organic cation. The thermal decomposition mechanism of the clay/organic complex is not clearly understood, but two quite distinct mechanisms have been proposed. Allaway[6] and Bradily *et al.*[7] assumed that the organic intercalant between the montmorillonite layers oxidizes in step-wise oxidation resulting in distinct weight loss after each step. According to the second theory proposed by Ramachadran *et al.*[8] and Aleshin *et al.*[9,10], two weight losses are observed at the heating stage. One at lower temperature is the oxidation of the organic molecule attached on the external montmorillonite surface and another at higher temperature due to oxidation of the intercalated organic molecule. As can be seen in Fig.3, $Ag(TBZ)_2$-montmorillonite showed a maximum carbon dioxide evolution rate around 400°C which does not coincide with the weight loss temperatures stated above. In the present work, however, only carbon dioxide evolution was examined. It is not unreasonable to assume that weight loss was caused by evolution of other kinds of gases. It is apparent that the thermostability of an organic compound is improved by intercalating between the montmorillonite layers. In turn, the thermostability of the montmorillonite layers is also improved by the carbon derived from the organic material after decomposition.

4. CONCLUSION

The structural modelling of montmorillonite intercalated with $Ag^+(TBZ)_2$ chelate has been performed by comparison of the observed and calculated intensities of (00*l*) reflections. Four different arrangements of the chelate between the layers of montmorillonite were considered. The results indicate that the $Ag^+(TBZ)_2$ chelate has its C-Axis perpendicular to the silicate layers. The montmorillonite intercalated by $Ag^+(TBZ)_2$ chelate has been prepared, and its thermostability was examined by using TG and CO_2 evolution analyses. The degradation temperatures of the TBZ and $Ag^+(TBZ)_2$ chelate were increased by intercalating between montmorillonite layers. The intercalated sample gave a maximum CO_2 evolution rate at around 400°C which did not coincide with the weight loss temperature.

ACKNOWLEDGMENTS

A part of the research was supported by a grant from the MITI, Japan. The authors wish to thank Topy Ind. Co. and Kunimine Ind. Co. for supplying clay minerals.

REFERENCES

[1] H.Favre, G.Lagaly, *Clay Minerals*, **26**, 19 (1991)
[2] F.Ohashi, A.Oya, *J. Clay Sci. Soc. Jpn.*, **37**, 58 (1997)
[3] K.Yvon, W.Jeitschko, E.Parthe, *J. Appl. Cryst.*, **10**, 73 (1977)
[4] M.J.Buerger, "Crystal-structure analysis", John Wiley & Sons, Inc., New York (1960) pp.585.
[5] S.H.Roy, "Fluorine micas", Bureau of Mines, Washington (1969) pp.113.
[6] W.H.Allaway, *Soil Sci. Soc. Am. Proc.*, **13**, 183 (1949)
[7] W.F.Bradley, R.E.Grim, *J. Phys. Colloid Chem.*, **52**, 1404 (1948)
[8] V.S.Ramachandran, S.P.Grag, K.P.Kacker, *Chem. and Ind.*, **23**, 790 (1961a)
[9] S.N.Aleshin, M.Sh.Schaimukhametov, *Dokl. Mosk. Sel'skokhoz. Akad.*, **64**, 75 (1961)
[10] S.N.Aleshin, M.Sh.Schaimukhametov, *Izu. Timiryazevsk. Sel'skokhoz. Akad.*, **2**, 37 (1962)

(Received December 16, 1999; Accepted May 6, 2000)